Available online at www.sciencedirect.com
ScienceDirect
Mendeleev Commun., 2016, **26**, 235–237
Mendeleev Communications

CuS nanoparticles synthesized by a facile chemical route under different pH conditions

Zamin Q. Mamiyev*[a,b,c] and Narmina O. Balayeva[a,c]

[a] *Institute of Physics, Azerbaijan National Academy of Sciences, AZ-1143 Baku, Azerbaijan*
[b] *Institut für Festkörperphysik, Leibniz Universität Hannover, D-30167 Hannover, Germany. Fax: + 49 511 762 4877; e-mail: mamiyev@fkp.uni-hannover.de*
[c] *Faculty of Chemistry, Baku State University, AZ-1148 Baku, Azerbaijan*

DOI: 10.1016/j.mencom.2016.05.004

The CuS/polymer nanocomposites were synthesized by a facile chemical route under different pH conditions, and the influence of pH on the optical and structural properties was studied by FT-IR, UV-VIS and photoluminescence spectroscopy, thermogravimetric analysis, atomic force microscopy and powder X-ray diffraction techniques.

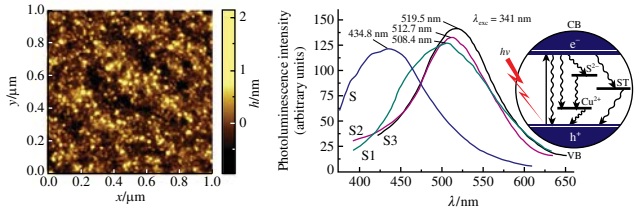

In the past decades, semiconductor metal sulfide nanoparticles (NPs) incorporated or impregnated on a polymer matrix have attracted significant interest because of their unique properties and wide application areas.[1–6] These nanostructures exhibit size-dependent properties such as a change of the electrochemical potential of band edge and an enhancement of photocatalytic activities with decreasing particle size.

Copper sulfides are promising semiconductor materials with various stoichiometric forms and valence states such as covellite (CuS) and chalcocite group compounds ($Cu_{2-x}S$) ($0 \leqslant x \leqslant 0.6$).[7] These compounds are stable at room temperature and widely used as p-type semiconductors with stoichiometry dependent optoelectronic properties.[3,4] Among them, CuS has been extensively applied to solar cell devices,[4,8] sensors,[5,9] catalysis,[10] nonlinear optical materials,[11] cathode material in lithium rechargeable batteries *etc*. Moreover, its unique properties are metal-like electrical conductivity and transforming into a superconductor at 1.6 K.[4] CuS also exhibits fast ion conduction at high temperature and other special characteristics for use in sensing are based primarily on its ability to promote electron transfer reactions with biomolecules.[12] CuS is an important p-type semiconductor with 2.2 eV direct band gap, which belongs to the wurtzite structure with vacancies within the lattice, providing its application in optoelectronic devices.[13,14] Due to its technological importance, the fabrication of CuS remains a main focus of interest to adopt new synthetic routes for obtaining phase pure material *via* economically and technically viable procedures. Numerous methods have been developed for the chemical synthesis of CuS nanostructures including hydrothermal technique, non-template free chemical route, sol–gel, chemical conversion, sonochemical, photochemical methods,[13–16] *etc*. However, some of the above methods use a salt of Cu^{2+} ions and H_2S, Na_2S, (CH_4N_2S), which are in separate phase and mixed unevenly, as well as assembling and aggregation of CuS particles are uneven. The precipitation of Cu^{2+} with S^{2-} is faster than their homogeneous mixing, the inhomogeneity at early stages results in a broadening size distribution. Therefore, for obtaining NPs with desired structures it is necessary to prevent the growth of the particle size with time.

A way to overcome this problem is the use of polymers as host materials to stabilize the NPs, avoid permanent aggregation, and this has attracted a lot of attention because of long-term stability and easily reprocessed ability of these materials.[17–19] Traditional methods usually have some drawbacks such as high temperature and/or high pressure, inert atmosphere protection, toxic organometallic precursors and it is difficult to grow controllable nanocrystalline materials under such conditions. Here we have applied a facile *in situ* method through simple chemical routes without any commitment to complex and toxic organometallic reactants to surmount many of these handicaps. The main characteristics of the MA/oct-1-ene copolymer (CP) are the absence of chemically active functional groups and/or atoms such as S, N, P and Cl along with its transparent appearance, high dimensional stability, ability to form films at room temperature, relatively high melting temperature, industrial inexpensive cost, and the specific stabilization activity of anhydride groups. Experiments were conducted at different pH values to evaluate the effects of reaction conditions on the optical and structural properties of CuS NPs.

The CP was synthesized from the relevant monomers by a radical copolymerization reaction in the presence of an initiator.[18,†] In the course of the reaction a greenish color was observed, which indicates the formation of CuS NPs. It was revealed that the increase in temperature leads to copolymer chain destruction, and the copper sulfide NPs cannot stabilize by small molecules of the copolymer. Hence, the particle size is growing irregularly and goes to beyond from nano size due to further aggregation, along with an irregular arrangement of particles in the CP matrix.

† The preparation of CuS NPs started with dissolving 1 g of CP in 96 ml of DMF in a 150 ml beaker followed by adding 0.459 g of copper(II) acetate to the solution, and the temperature was slowly increased up to 80 °C with constant stirring. The sulfur precursor solution (0.072 g of thiourea in 4 ml of DMF) was added dropwise and the pH was maintained at 9.5, 10.0 and 10.5 by adding a 20% solution of NH_4OH (hereinafter S1, S2, and S3, respectively). All of the synthesis experiments were conducted in a flask equipped with a water-cooled condenser and a magnetic stirrer.

As it is known nanocrystals (NCs) grow *via* nucleation and a subsequent growth stage. Regarding the formation of metal sulfide NPs, Cu^{2+} cations were absorbed by the polymer through weak bonds to functional groups.[20] Further thiourea produces S^{2-} anions in the solution and the formation of colloidal CuS starts with an interaction between two ions. In this case, size of the formed NPs exactly depends on the metal atoms loaded in a polymer matrix and S^{2-} anions concentration. Since the reaction rate jumps up owing to increase in the amount of S^{2-} ions by extending alkali medium, we can control the grain size by managing the pH value. The optimum condition for CuS NPs formation appears to be pH 9.5 in this experiment. Therefore, the smaller grains are structured in the polymer matrix due to balanced supply of Cu^{2+} and S^{2-} ions at this pH. The formation of CuS can be described by the following reaction stages:

$$2\,Cu(AcO)_2 \rightarrow 2\,Cu^{2+} + 4AcO^-,$$

$$(NH_2)_2CS + OH^- \rightarrow CH_2N_2 + H_2O + SH^-,$$

$$SH^- + OH^- \rightarrow S^{2-} + H_2O,$$

$$Cu^{2+} + S^{2-} \rightarrow CuS\downarrow.$$

The initial factor responsible for the final morphology of the products is the crystallographic phase of the seed formed during the nucleation process, which depends on the nature of the material and on the environmental conditions. Since the reaction time has a remarkable influence on the nucleation process, it was maintained at 5 h for all of the syntheses. It is considered that the cavities in the polymer matrix provide a certain stabilization of the MeS NPs. Moreover, the stabilization of additional NPs becomes feasible through oxygen atoms and double bonds in the polymer molecule.[21,22] The same physical conditions were kept stable during the synthesis. The powder and films thus obtained after the evaporation of solvents were dried in a vacuum furnace at 45 °C for 48 h to remove any entrapped solvent.

The FT-IR spectra for the CP and PNC (S1) were recorded at room temperature in a region of 400–4000 cm^{-1} using KBr pellets [Figure 1(*a*)]. Both spectra exhibit characteristic bands of stretching and bending modes for O–H, C–H, H–C–H, C=O, and C–O groups with identical noticeable shifts. The peaks at 669 and 925 cm^{-1} correspond to the bending vibrations of C–H in the copolymer chain. The bands at about 1024 and 1716 cm^{-1} are due to the C=O stretching vibration. The stretching and deformation vibration peaks around 1186 and 1242 cm^{-1} can be explained by the C–O–C vibrations. The band corresponding to CH_2 asymmetric stretching vibrations occurs at about 2860–2965 cm^{-1}, and a sharp band at 1458 cm^{-1} is assigned to CH_2 scissoring vibrations.[22–24]

The intensity changing and shifting are observed with the formation of CuS NPs as depicted in curve *2* [Figure 1(*a*)],

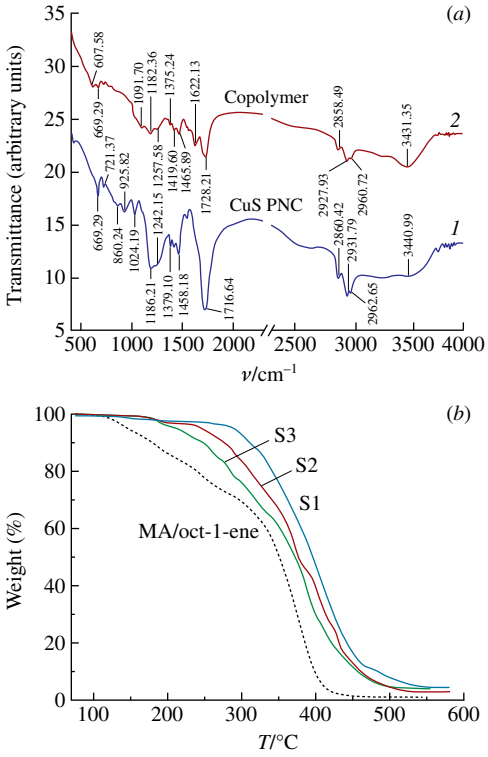

Figure 1 (*a*) FT-IR (for S1) and (*b*) TGA spectra for the CP and as-synthesized CuS PNCs.

which proved the interaction between CuS and polymer chain. Therefore, van der Waals interaction between functional groups and the surface of particles provides the stability of NPs. The band at 608 cm^{-1} was attributed to the characteristic signals of valence oscillations of Cu–S bonds. Additional weak bands were observed in this area to indicate the presence of resonance interaction between the vibration modes of sulfide ions in a crystal.

Thermal behavior of nanocomposites is an important property for the construction of materials to be used in specific fields. In this respect, the size and dispersion of NPs in the polymer matrix has a significant contribution in tailoring the thermal properties.

From TGA curves, it is identified that CP starts to decompose at 120 °C [Figure 1(*b*)]. However, in the case of nanocomposites, this temperature tends to increase with the formation of NPs. Hence, it can be inferred from the line S1 where decomposition temperature gets bigger value and progressed on the roughly straight line contributed to the formation of smaller NPs with a narrow size distribution. This is due to the stronger interfacial interaction between the polymer backbone and relatively small CuS NPs, which ultimately leads to the restriction of polymer chain mobility.

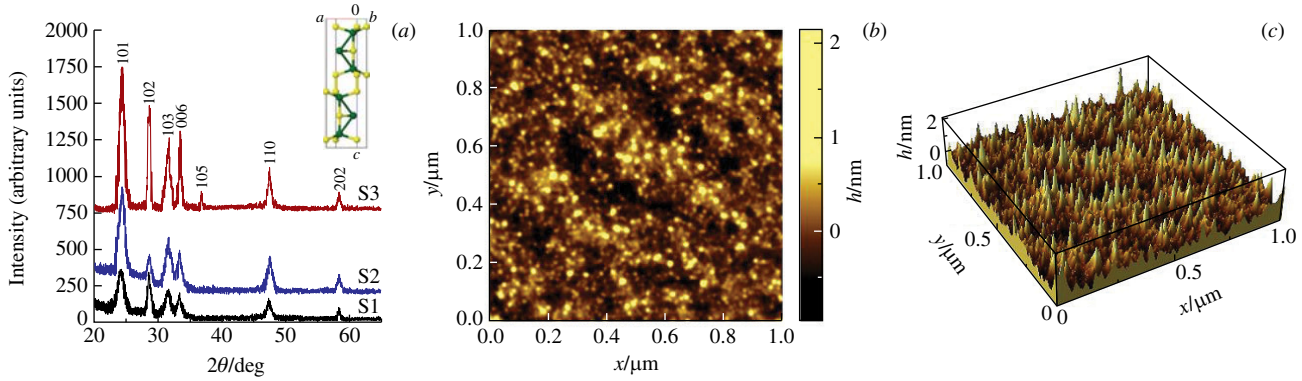

Figure 2 Powder XRD patterns and AFM images (S1) of composited CuS NPs.

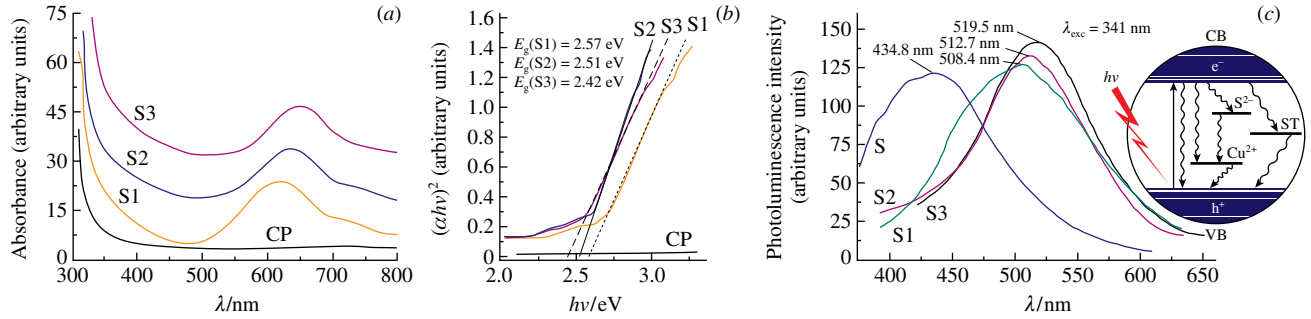

Figure 3 (*a*) Absorption spectra, (*b*) Tauc plot and (*c*) PL spectra for CP and CuS PNCs in DMF (the inset depicts energy level diagram in CuS).

The phase purity and crystallinity of the synthesized CuS NPs were examined on a powder X-ray diffractometer operated at 40 KeV and 40 mA with a scanning rate of 0.02° using Ni-filtered CuKα radiation (λ = 1.5406 Å). The diffraction peaks (Figure 2) can be assigned to the hexagonal structure of CuS (covellite phase) with JCPDS no. 06-0464, corresponding space group of $P6_3/mmc$ and calculated lattice parameters a = 3.745 and c = 16.518 Å. No other peak pointing out the CuS phase was identified from XRD measurements. The broadening of XRD lines is associated with a small particle size of coherently diffracting crystallites. According to the Scherrer formula,[25] the calculated average crystallite sizes were 5.7, 7.5, and 9.2 nm for S1, S2, and S3, respectively.

Figure 2 shows the two- and three-dimensional AFM images of CuS NCs on the copolymer matrix (S1). The films were prepared on a glass substrate with the homogeneous surface with the deposition of the produced solution. All measurements were performed under ambient conditions. The average size was estimated at about 6 nm, which is in good agreement with the XRD and UV-VIS results. AFM images present almost well-distributed NPs on the CP matrix and this should be considered the ordinary case for the method used.

Metal sulfide NPs possess optical properties that are sensitive to size, shape, concentration, agglomeration state and refractive index near the nanoparticle surface, which makes UV-VIS and PL spectroscopy a valuable tool for studying these materials. When semiconductor NCs become smaller than the exciton radius, they exhibit a threshold energy in the optical absorption measurements because of size specific band gap structures, which is reflected by the blue shift of the absorption edge. On the other hand, the wavelength increases with the broadening of the particle size distribution.[5] Figure 3(*a*) displays the UV-VIS absorption spectra of the CP and PNCs solutions in DMF recorded at room temperature in a 300–800 nm spectral range. The synthesized NPs manifest a wide length and strong absorption between 550–650 nm under all the pH conditions. Therefore, well-defined exciton absorption feature around 620 nm in near-IR regions is characteristic of CuS. In all the cases, the absorption edge shows a slightly red shift corresponding to that of the bulk CuS, which may be due to quantum confinement effects. We did not observe any absorption shoulders at 430–460 nm corresponding to the Cu_2S phase, which proved that the sample contained a pure covellite phase. The optical band gap energy (E_g) of the CuS NCs was calculated using the Tauc plot [$(\alpha h\nu)^n$ = = $A(h\nu - E_g)$, where α is the absorption coefficient, $h\nu$ is the photon energy, A is a constant, and n is either 1/2 for an indirect transition or 2 for a direct transition] with extrapolating the linear portion of the curve to the x axis, Figure 3(*b*).[26]

According to the PL spectra, there is a sharp rise starting at about 460 nm, which is clearly blue shifted with respect to bulk covellite considering band to band transition and corresponds to room temperature band gap energy for the CuS NCs. The initial maximum wavelength at 508 nm for S1 slightly shifts as the pH value is changed. The pure CP gives a PL peak at around 434 nm [Figure 3(*c*), S] despite it does not display any absorption feature in the UV-VIS spectrum [Figure 3(*a*)]. However, as against the expectations the shoulder disappears in nanocomposite PL curves but obviously supports its expansions. The energy states within the band gap in the NCs are revealed because of surface states, defects, and/or Cu^{2+} or S^{2-} ions. The impinging photons with higher energy excite the electrons from the Cu^{2+} levels or a valence band (VB), which reached the conduction band (CB). Afterward, the excited electrons decay non-radiatively to surface states (ST) and then decay radiatively to VB and emit lower energy photons. When the particle size decreases to nanosize, the VB edge shifts downwards. Therefore, the emitted photons have comparatively higher energy and give a blue shift in the PL curves.

References

1 F. Henneberger, J. Puls, Ch. Spiegelberg, A. Schulzgen, H. Rossman, V. Jungnickel and A. I. Ekimov, *Semicond. Sci. Technol.*, 1991, **6**, A41.
2 S. Lindroos, A. Arnold and M. Leskelä, *Appl. Surf. Sci.*, 2000, **158**, 75.
3 L. D. Partain, P. S. McLeod, J. A. Duisman, T. M. Peterson, D. E. Sawyer and C. S. Dean, *J. Appl. Phys.*, 1983, **54**, 6708.
4 Y. J. Yang and J. W. Xiang, *Appl. Phys. A*, 2005, **81**, 1351.
5 Z. Q. Mamiyev and N. O. Balayeva, *Chem. Phys. Lett.*, 2016, **646**, 69.
6 V. Klimov, P. Haring Bolivar, H. Kurz, V. Karavanskii, V. Krasovskii and Yu. Korkishko, *Appl. Phys. Lett.*, 1995, **67**, 653.
7 K. Tezuka, W. C. Sheets, R. Kurihara, Y. J. Shan, H. Imoto, T. J. Marks and K. R. Poeppelmeier, *Solid State Sci.*, 2007, **9**, 95.
8 R. S. Mane and C. D. Lokhande, *Mater. Chem. Phys.*, 2000, **65**, 1.
9 X. Zhang, G. Wang, A. Gu, Y. Wei and B. Fang, *Chem. Commun.*, 2008, **45**, 5945.
10 Y. Wang, Q. Li, M. Nie, X. Li, Y. Li and X. Zhong, *Nanotechnology*, 2011, **22**, 305401.
11 H. L. Xu, W. Z. Wang and W. Zhu, *Mater. Lett.*, 2006, **60**, 2203.
12 Y. Huang, H. Xiao, Sh. Chen and Ch. Wang, *Ceram. Int.*, 2009, **35**, 905.
13 N. O. Balayeva, O. O. Askerova, A. A. Azizov, R. M. Alosmanov, G. M. Eyvazova and M. B. Muradov, *Composites Part B*, 2013, **53**, 391.
14 Y. C. Zhang, X. Y. Hu and T. Qiao, *Solid State Commun.*, 2004, **132**, 779.
15 M. Urbanová, J. Kupčík, P. Bezdička, J. Šubrt and J. Pola, *C. R. Chim.*, 2012, **15**, 511.
16 H. Wang, J. R. Zhang, X. N. Zhao, S. Xu and J. J. Zhu, *Mater. Lett.*, 2002, **55**, 253.
17 J. Schmitt, G. Decher, W. J. Dressick, S. L. Brandow, R. E. Geer, R. Shashidhar and J. M. Calvert, *J. Adv. Mater.*, 1997, **9**, 61.
18 Z. Q. Mamiyev and N. O. Balayeva, *Opt. Mater.*, 2015, **46**, 522.
19 O. O. Akinwunmi, G. O. Egharevba and E. O. B. Ajayi, *J. Modern Phys.*, 2014, **5**, 257.
20 K. G. Kanade, R. R. Hawaldar, R. Pasricha, S. Radhakrishnan, T. Seth, U. P. Mulik, B. B. Kale and D. P. Amalnerkar, *Mater. Lett.*, 2005, **59**, 554.
21 L. Chu, B. Zhou, H. Mu, Y. Sun and P. Xu, *J. Cryst. Growth*, 2008, **310**, 5437.
22 N. O. Balayeva and Z. Q. Mamiyev, *Mater. Lett.*, 2016, **162**, 121.
23 G. H. Hu and H. Cartier, *J. Appl. Polym. Sci.*, 1999, **71**, 125.
24 Z. Q. Mamiyev and N. O. Balayeva, *Composites Part B*, 2015, **68**, 431.
25 P. Scherrer, *Nachr. Ges. Wiss. Göttingen*, 1918, **26**, 98.
26 J. Tauc, *Amorphous and Liquid Semiconductors*, Plenum Press, London, 1974.

Received: 3rd November 2015; Com. 15/4766